Pulsar Spin Down Luminosity

December 6, 2022

Abstract

Pulsars and their associated Pulsar Wind Nebulae (PWNe) are complex astrophysical systems that have been widely studied. The exact relationship between PWNe (which is easy to observe) and Pulsars needs to be characterized well in order to fully understand the dynamics of the system. In this paper, we follow on previous work by studying the relationship between the rate of observed energy loss of a pulsar - as seen in a slowing of the pulsar's rotational speed - to the luminosities of the PWNe that surround them. We find there is a roughly linear relationship between the two quantities, but our model is too simplistic to fully account for all energy transfer processes.

1 Introduction

Neutron Stars were first suggested as an endpoint of stellar evolution in 1934, with researchers believing they may occur in supernova remnants. Indeed, Neutron Stars are very dense stellar remnants that are made mainly of neutrons [2]. Pulsars are neutron stars that release beams of radio emission continuously in a very specific direction. This radio emission appears to observers as oscillating to an outside observer. Because the beam is only visible when the beam is pointed at the observers, they appeared to be pulsing to observers (thus the name). The pulsing radio signal phenomena was first observed and linked to the rotations in neutron stars by Hewish et. al. in 1968 [9].

One of their most striking observations about pulsars was the consistency with which the neutron stars appeared to pulse. Initially, they found the period of oscillation to be constant to 1 part in 107, and modern research can now show the pulses to be constant up to one part in 10^{-16}. This incredible precision is nearly the same as modern day atomic clocks [7]. Neutron stars have a very large moment of inertia, so it makes sense why they would be difficult to spin up or down.

Being very exotic in their properties, Pulsars are both interesting in their own right and extremely important in understanding fundamental physics. The extreme densities and magnetic fields of neutrons stars make them excellent examples and windows into topics such as high magnetic fields and General Relativity [11]. For the better part of a century, astronomers have been studying the prototypical Pulsar example - the Crab Pulsar. A significant amount of this research has been dedicated to understanding the spectrum of its surrounding Wind Nebulae and source of power of the wind nebula, paying special attention to the Crab Neula [13]. It is important to understand the connection between Pulsar Wind Nebula (PWN) and the pulsars they contain because it may be useful to use the nebula as a proxy to study the pulsar [17]. Here, we wish to continue this work by examining the relationship between the spin down luminosity of pulsars and the observed luminosity of the surrounding wind nebulae. This work is particularly timely, as recently data from the HESS Galactic Plane Survey (HGPS) has shown a whole host of new pulsars to study. The survey was able to find over 70 high intensity objects, including PWNe [1].

1.1 Pulsar Properties

A basic understanding of pulsar dynamics is required to fully appreciate how pulsars serve as power plants for their surrounding nebula. The relationship between density and period is important, and can be stated rather simply in eq. 1:

$$\rho = \frac{3 * \pi}{G * P^2} \tag{1}$$

where ρ is the density, G is the gravitational constant, and P is the period of the Pulsar. Given a period of $P = 0.033s$ for the Crab Pulsar (M1), one can estimate the density of the pulsar to be $10^8 cm^{-1}$ [7]. Additionally, the relationship between mass, period and radius is given by [7]

$$R < (\frac{GMP^2}{4\pi^2})^{1/3} \tag{2}$$

Given a few observable parameters, one can characterize the rest of the pulsar. Since several parameters are needed to fully describe a pulsar it is easier to look at the standard example. Traditionally, a 'canonical pulsar' is defined to have approximately the average characteristics of a Pulsar based on pulsars we have so far observed. The canonical pulsar has the following characteristics [7]:

1. $P = 1.4 * 10^{-3}$
2. $M = 1.4 * M_\odot$
3. $R = 10$ km
4. $I = 10^{45} gcm^2$

The Crab Nebula Pulsar - of particular interest in this paper - corresponds closely to these numbers.

In Addition to having very high densities and constant periods, Pulsars also have very strong magnetic fields. These magnetic fields are usually on the order of 10^{12} Gauss. These large magnetic fields also lead to a rather strong dipole moment. In general the axis of rotation of a Pulsar is not going to be the same as the as the direction of the dipole moment. This leads to magnetic dipole radiation, given by [7]:

$$P_{rad} = \frac{2}{3c^2}(BR^2 \sin\alpha)^2(\frac{2\pi}{P})^2 \tag{3}$$

Where P_{rad} is the power given off, P is the period, B is the magnetic field strength at the surface, R is the radius and α is the inclination angle. The magnetic dipole radiation of known pulsars, based on observed rotational rates, has relatively low frequency. This frequency is not high enough to be observed from earth as it gets absorbed by the surrounding SNR Nebula. This energy is absorbed by the surrounding nebula and re-emitted as radiation - one of the ways the nebula can gain energy as well as through a wind of relativistic charges particles and Synchrotron Radiation [17]. It is useful to quantify this energy loss by examining how fast the pulsar is loosing kinetic energy (see eq. 4). Though pulsars do spin at a very constant rate, this rate shifts over time as the pulsar looses energy.

$$E = \frac{2\pi I^2}{P^2} \tag{4}$$

The energy is related to the moment of inertia and the period of the neutron star. As the pulsar gives up energy, the moment of inertia (i.e. the period) of the pulsar must decrease. The spin down rate is an easily measurable quantity with a modern radio telescope. The observation that pulsars tend to spin down over time is known as 'pulsar braking' [7]. Pulsars spin at a very constant rate, and so one might think the amount of energy radiated is negligible. The stars carry so much energy that a small relative change in moment of inertia is still quite a lot of energy. The specific amount of energy that is lost is given by [7]:

$$-\dot{E} = L_{spindown} = \frac{4 * \pi^2 I\dot{P}}{P^3} \tag{5}$$

Where $L_{spindown}$ is the spin down luminosity of the pulsar. The term 'spin down luminosity' refers to the fact that the loss of rotational energy leads to the nebula absorbing energy - which it then radiates and is observable as a luminosity. The spinning down of the pulsar effectively powers the surrounding nebula. One easy way to quantify how much energy is lost is by a breaking index. The breaking index is defined by relating the current angular velocity of the pulsar to its derivative. Using n as the braking index [7]:

$$\Omega = C * \dot{\Omega}^n \tag{6}$$

or in terms of the period and derivative of the period:

$$n = 2 - \frac{P\ddot{P}}{\dot{P}^2} \tag{7}$$

This relation for spin down luminosity - and how we characterize the spin down of pulsars - is simple and intuitive. It may not be the entire picture, however. Relativistic computational simulations are able to show that spin down luminosity may require more work to fully explain the phenomena. Since the mechanism by which the pulsar looses energy is primarily related to magnetic dipole radiation, a relativistic approach must be taken to get the most accurate results [15]. Experimentally, this discrepancy has been observed in the x-ray regime. There is a strong correlation between the theoretical spin down luminosity of the pulsar and the emission of the surrounding wind nebula, indicating that magnetic dipole radiation is where a large amount of this energy is coming from. But the relation in 5 was found to be imperfect, indicating that additional parameters need to be considered [14]. While the equation may be imperfect, the total amount of luminosity visible directly from the radio pulses is about one percent [10] so the majority of the energy given off by the pulsar should go into the Nebula Surrounding the Pulsar. The simple magnetic dipole moment model is an approximation for the more complex energy transfer process and will be used.

1.2 Pulsar Wind Nebula

Surrounding some Pulsars are Pulsar Wind Nebulae (PWNe), a magnetized particle wind. This is where the energy from the pulsars can be dumped before being radiated. The PWNe are easily observable with a telescope. One example is shown in fig. 4 of the crab nebula. The pulsars with PWNe can be compared to other supernova remnants (SNRs) with shell like structures. Shell like SNRs gain most of their energy from the initial supernovae, compared to PWNe which primarily get their energy from the Pulsars they contain [8].

Just after the supernova, a PWNe supersonically expands, shocking the surrounding gas. A reverse shock is formed, and will reverberate several times in the nebula until a more steady, sub-sonic expansion phase begins. At this point, the shock heated gas in the nebula is powered by the Pulsar inside. The energy from the Pulsar - and thus the PWNe - remains constant for a time and then begins the decrease. The time at which the power begins to decrease is given by [8].

$$\tau_0 = \frac{P_0}{(n-1)\dot{P}_0} \tag{8}$$

where n is a constant and P_0 and $\dot{P}_0$ are the initial period of rotation and its derivative. After the initial expansion, the evolution of the PWNe can be roughly described by a simple expansion relation: $R \propto t^{2/5}$ in the steady state expansion Sedov-Taylor regime [8]. The exact shape and nature of the nebula is highly dependent on both the original supernova, and the ISM in which the remnant is expanding [8]. The conditions inside PWNe can be extreme, with very high temperatures. Additionally, the rate at which energy is released from the PWNe is far from constant even if the rate of energy loss from the pulsar is constant. For instance, others have observed significant γ-ray flares from the Crab Nebula. These flares caused an order of magnitude increase in γ-ray flux for a few hours [5]. The dynamics of pulsars and PWNe are extremely complex, and we are only characterizing them in a simplified way. We anticipate from the outset significant systematic errors in our data.

To better understand energy loss in pulsars - and verify the assumption of magnetic dipole radiation powering the surrounding nebulas - we will look at the total observed power output of a specific SNR and compare that to the spin down luminosity based on the observed rotational rate and derivative of the rotation rate. Specifically, we will be looking at the Crab Nebula and associated Pulsar (known as M1 and PSR B0531 +21 respectively). They are very well documented objects and similar to the canonical pulsar, making the pair a good test system. We then use several external data sets to examine the relationship between pulsars and PWNe over a variety of pulsars. This second approach gives us the opportunity to use more precise and varied data.

2 Experimental Methods

2.1 Crab Pulsar Luminosity

Initially, as a proof of concept, we calculate the luminosity of the Crab Nebula - also known as M1 - to compare to the spin down luminosity of the pulsar contained within it. Images of M1 were obtained using the Los Cumbres Observatory (LCO) telescope network. The telescope itself is in Tenerife. It is a 0.4 meter telescope with SBIG STL6303 sensor. The telescope parameters and other hardware details can be found at the LCO's Website (https://lco.global/).

10 images in both filter bands were taken. The images were processed using DS9 to turn them from .fz files to regular .fits files. They were subsequently aligned and averaged using astroart to generate an average

image in each bandpass. This improves S/N. Bessel B and V filters were chosen because of availability of the filters and availability of reference star data. We could not find any suitable reference stars in the sdss filters, so we were restricted to the two Bessel filters available for our instrument. Both filters are used to get a color temperature, and only one is required to find an estimate for luminosity.

Total flux (in ADU) was calculated simply by adding up the total value of all pixel in the nebula. The average background value was then subtracted off to compensate for errors and background flux. The flux in ADU of G 100-20 was also found. Using the star as a reference magnitude for the B band, and HD 245010 for the B band [19], one can calculated the magnitude of M1 in a specific bandpass:

$$m_{M1} - m_{Star} = ln(F_{M1}/F_{Star}) \tag{9}$$

This gives a relative magnitude of M1 and the reference star. Since the reference star's magnitude is already known, this allows us to find the magnitude of M1. This magnitude then needs to be converted into an absolute magnitude as given in equation 10:

$$M = m + 5 - 5 * log_{10}(distance) \tag{10}$$

The flux for a given magnitude in each band is known according to [4]. This can then be used to find the flux (in our desired unit) of an object whose magnitude is known.Using F_1 and F_2 for the fluxes of the two objects:

$$\frac{F_1}{F_2} = 10^{0.4*(M_2 - M_1)} \tag{11}$$

Where F_1 is the magnitude of the Crab Nebula, and F_0 is the flux corresponding to zero magnitude (i.e. $M_2 = 0$) [4]. Now that the flux in a given band pass is known, it is relatively straight forward to calculate the luminosity. If you assume the object is giving out energy equally in all directions, you just have to multiply by the surface area of the sphere to get the total luminosity given by an object in a specific band. In order to get a bolometric luminosity, one needs to repeat this procedure for every wavelength. While theoretically this could be done with a large number of filters in a large number of frequency bands, finding all of those luminosities is impractical. Instead, we only use one filter, the Bessel B filter. We use the observed luminosity in one bandpass to 'calibrate' a full spectra of the object. In other words, the spectral distribution is integrated over the desired frequencies to find the percentage of the distribution can pass through the B filter. The observed luminosity is then taken to be equal to that percentage of the total luminosity. More concretely:

$$L_{total} = \frac{\int_{\infty}^{\infty} f(\nu)\, d\nu}{\int_{\infty}^{\infty} f(\nu) * S(\nu)\, d\nu} * L_B \tag{12}$$

where $f(\nu)$ is the function describing the distribution of the flux from the nebula in terms of wavelength. $S(\nu)$ is the sensitivity function of the Bessel B filter. For simplicity, we approximate $S(\nu)$.

$$S(\nu) = \begin{cases} 1 & 380 < \nu < 490 \\ 0 & \text{otherwise} \end{cases} \tag{13}$$

Where ν is measured in nanometers. This makes one component of the integral rather simple. Describing the spectra in an integrable way, however, is far from easy.

2.2 Crab Nebula Spectra

Finding an analytic expression for the spectral distribution function of the crab nebula is required to appropriately calibrate the Luminosity. The experimental distribution is given by fig. 1. Often, the spectra of a PWNe can be described by a power law function:

$$f(\nu) \propto \nu^{-\alpha} \tag{14}$$

Where α is a function of wavelength itself [18]. This expression is simple, but due to the variability of α is not the most useful computationally. Much work has been done to understand the crab nebula spectra, especially its more unusual bumpy features. This work is often confined to narrow wavelength bands (with a healthy use of piece wise functions), so finding an accurate description of the spectra accross all wavelength bands proved challenging. Due to the this complexity, we took a different less precise approach.

Instead, one can assume the Crab Nebula is approximately a black body. Using the B / V filters, we can construct an effective temperature. The equation for effective temperature (ignoring matallicity) can be described approximately as:

$$\log T_{eff} = c_0 + c_1(B - V) + c_2(B - V)^2 + c_3(B - V)^3 \tag{15}$$

where the constants being given in [16]. From this effective temperature, a black body spectrum is easily found.

$$f(\nu) \propto \frac{\nu^3}{c^2} \frac{1}{\frac{h\nu}{ek_B T} - 1} \tag{16}$$

Where T is the effective temperature. This is not an ideal way to estimate the bolometric luminosity.

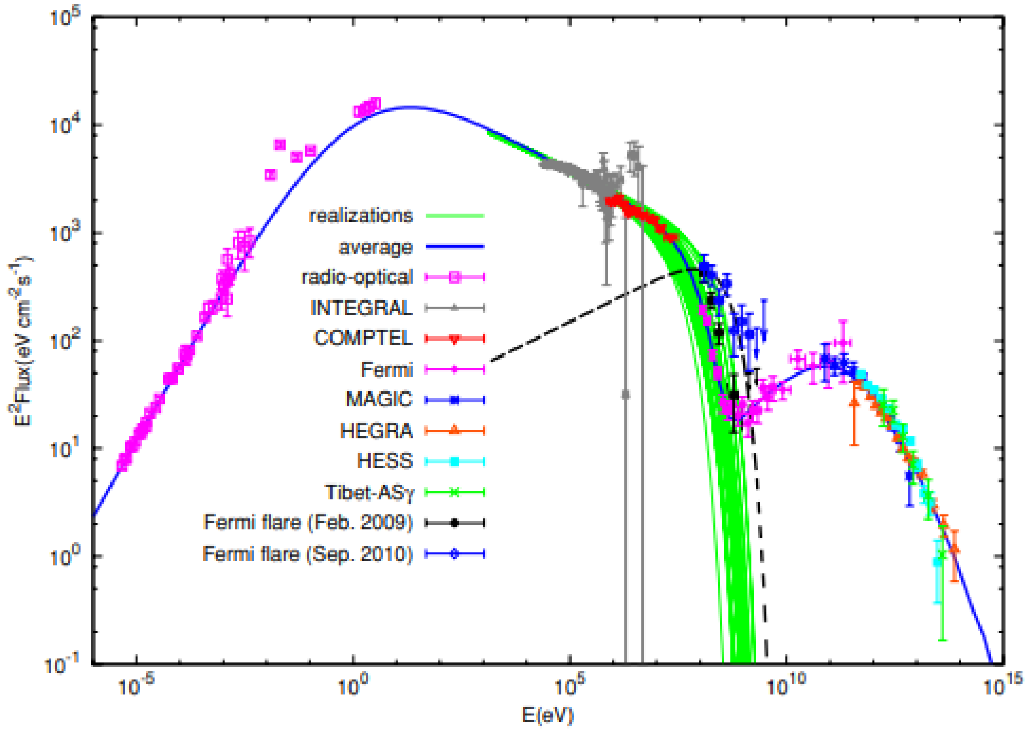

Figure 1: Spectrum of the Crab Nebula across 20 energy orders of Magnitude. Each color represents a different data source. The spectra shows the Crab Nebula is much more complex than a simple blackbody [20]

This is because of the narrow band of actual light observed and the simplification of the Spectral Distribution Function for the Crab Nebula. Both of these sources of systematic error indicate that the resulting luminosities are most useful as an order of magnitude estimate of the Luminosity.

This was not the only option available, but rather the most feasible option given the experimental resources on hand. The most straightforward way to calculate luminosity is to use the images - and the camera parameters - to count the number of photon hits on the sensor. This can then be fairly easily extrapolated over the entirety of the nebula, gving the flux, and therefore luminosity, in the desired band. Do this over enough filters, and a very good estimate of the nebula's Luminosity is possible.

While this is the most direct way, it is certainly not the most practical. Some of the data taken at the Los Cumbres Observatory is pre-processed, and so accurate photometric flux calculations will be inaccurate. Additionally, we have a limited number of filters, so the majority of the photons would not have the right frequency to be counted. Lastly, in the filters that were available suitable reference stars with magnitudes also in our filters was a challenge to find. All of these factors combined to make it impractical to calculate the Luminosity so directly. The less direct approach we are taking is the more reasonable method to use.

```python
for i in range(len(arr)-1):

    j = 0
    try:
        while arr[i][j] != sp:
            j += 1
    except IndexError:
        j = j - 1

    k = 9
    try:
        while arr[i][k] != sp:
            k += 1
    except IndexError:
        k = k - 1

    if arr[i][0:j] == 'PSRJ':
        PSRJ_arr.append(arr[i][9:k])
    if arr[i][0:j] == 'RAJ':
        RAJ_arr.append(arr[i][9:k])
    if arr[i][0:j] == 'DECJ':
        DECJ_arr.append(arr[i][9:k])
    if arr[i][0:j] == 'POSEPOCH':
        POSEPOCH_arr.append(arr[i][9:k])
    if arr[i][0:j] == 'F0':
        F0_arr.append(arr[i][9:k])
    if arr[i][0:j] == 'F1':
        F1_arr.append(arr[i][9:k])

```

Figure 2: Data scraping algorithm

2.3 Spin Down Luminosity

Finding the observed luminosity of M1 is only half the project, the other half coming from a survey of a wide range of pulsars and PWNe. We used data obtained from the Australia Telescope National Facility Pulsar Catalog (ATNF PSRCAT). Much of the data in this catalog comes from the ATNF's Parkes Radio Telescope, a 64 meter telescope Located in New South Wales. The full specifications of this instrument can be found on their website (https://www.atnf.csiro.au/research/pulsar/index.html) [12]. This catalog contains all the necessary parameters (i.e. P and $\dot{P}$) for over 2000 different pulsars. It also includes uncertainties. The spin down luminosities are then calculated using equation 5. All errors were propagated using standard error propagation.

We wanted to take this database and be able to extract certain pulsar parameters to compare to other external data sources. Getting the data into a usable form proved tricky, however. One of the initial problems was that the ATNF data was stored on their website in HTML as text, instead of in a table as is normal. This meant that off the shelf web scraping programs such as BeautifulSoup would not work.

We made a custom python code to get our data into a usable form. A snippet of the code can be found in fig. 10, 3. We downloaded the entire ATNF database in a .db form and made it into a txt files. Then we

```
for i in range(len(arr)-14):
    #print(arr[i])
    j = 0
    try:
        while arr[i][j] != sp:
            j += 1
    except IndexError:
        j = j - 1
    #print(j)
    k = 9
    try:
        while arr[i][k] != sp:
            k += 1
    except IndexError:
        k = k
    #print(k)
    l = i+1
    PulsarLabels_arr = []
    Pulsar_arr = []

    if arr[i][0:j] == 'PSRJ':
        PSRJ_arr.append(arr[i][9:k])
        PulsarLabels_arr.append(arr[i][0:j])
        Pulsar_arr.append(arr[i][9:k])
        while arr[l][0:j] != '@---' :
            m = 0
            n = 9
            try:
                while arr[l][m] != sp:
                    m += 1
            except IndexError:
                m = m - 1
            try:
                while arr[l][n] != sp:
                    n += 1
            except IndexError:
                n = n
            PulsarLabels_arr.append(arr[l][0:m])
            Pulsar_arr.append(arr[l][9:n])
            if l < len(arr)-2 :
                l += 1
            else:
                break
    if PulsarLabels_arr != [] :
        Labels_arr.append(PulsarLabels_arr)
    if Pulsar_arr != [] :
        Data_arr.append(Pulsar_arr)
```

Figure 3: Snippet of code displaying creation of the Labels and Data arrays in the data manipulation part of our code.

used the code in fig. 10 to look through the whole txt file and output names and parameters. As part of this, we had to account for the fact there may be a mismatch in the spacing of the name to the parameter. In other words, if some Pulsars did not have a parameter, no value would be added so there would be a mismatch in the position in the list of each parameter. Once this was accounted for, the data could be further analyzed. In addition to writing a script to grab a certain parameter and the corresponding pulsar, we also wrote a script to sort and otherwise manipulate the pulsar data (Fig.3). In the ATNF catalogue, we are only given F and $\dot{F}$, where F is the pulsar's frequency. To account for this, we re-arrange our previous expression for spin-down luminosity so that it is in terms of the frequency for actual calculation:

$$\dot{E} = 4 * \pi^2 I F \dot{F} \tag{17}$$

Where I is the moment of inertia (from the canonical pulsar).

Finding the observed Luminosities was significantly more difficult. A database is needed, because it is impractical for us to calculate the total luminosity of a nebula as done in the previous section for a large number of PWNe. We searched for a complete database, but did not find any comprehensive resource. One issue with the search was often sources would have high errors or only report on a limited number of PWNe. We wanted something more complete and with low error, for more consistency and more accurate systematic error analysis.

For PWNe data, we used [3]. This paper was mainly focused on the x-ray band, using the ROSAT and ASCA telescopes. Specifically, they were interested in understanding the dynamics of radiation in the x-ray regime in PWNe. [3] provided both bolometric and x-ray luminosities. We expect the x-ray luminosities to be significantly different than the spin down luminosity due to it not covering all possible wavelengths. To avoid systematic errors, we decided to focus on the relationship between spin down luminosity and observed luminosity instead of focusing on comparing absolute values. If all of the energy from the pulsar is going into the wind nebula, then we would expect the graph of those two parameters to be a line with a slope of one. A different slope would tells us about the conversion factor (i.e. the fraction of energy absorbed). If the relationship is non-linear, or the slope is very small, than our hypothesis of the pulsar powering the surrounding PWNe is most likely incorrect.

It is important to note that for the x-ray data we compiled, the luminosities are the luminosities of the total region. In other words, it could include luminosity deriving directly from the pulsar. While this is not ideal, to a good approximation, all of the flux in the x-ray regime is coming from the PWNe [6]. Additionally, we were able to get data pertaining to both a spin down luminosity, called *Calculated Energy Loss* and direct measurement of the pulsar energy loss, termed *Accepted Energy Loss* for the remainder of this work.

Figure 4: Image of the Crab Nebula (M1) in the B filter bandpass.

3 Results

Fig. 4 and fig. 5 shows the images of the Crab Nebula that we used to calculate color temperature and calibrate the spectrum. The flux in ADU for the Crab Nebula was about $5.8 * 10^6$ in the Bessel B filter. Using [19] for the magnitude of G100-20, the final calculated magnitude was $m = 13.6$. This lead to an absolute magnitude of $M = 7.11$ and a luminosity of $L = 2.8 * 10^{33}$ erg.

The the percentage of the flux that is in the Bessel B pass band is given by taking the integrals in Eq. 12 of the given distribution function and filter sensitivity function. In the end this results in a total luminosity (in erg/s) of:

$$L_{total} = 2.0 * 10^{34} \tag{18}$$

This is compared to the value the ATNF found of $L_{Spindown} = 4.5 * 10^{38}$. The relative error on this measurement was about 370 percent. This is significantly different than the value we calculated. Initially, error was determined using the read noise of our instrument. Errors were then propagated through the calculations using standard error propagation formula. The spectra was assumed to be exact, but significant errors can be found in the spectra both because of its incorrect shape and errors finding the color temperature.

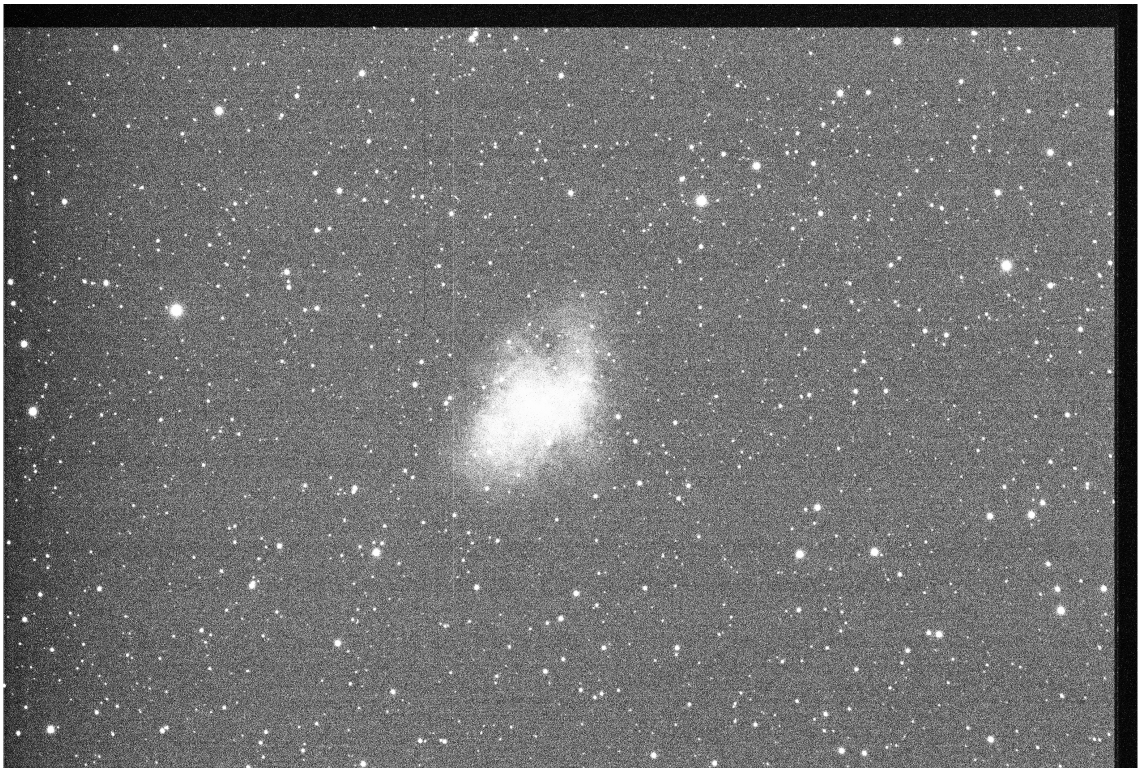

Figure 5: Image of the Crab Nebula (M1) in the V filter bandpass.

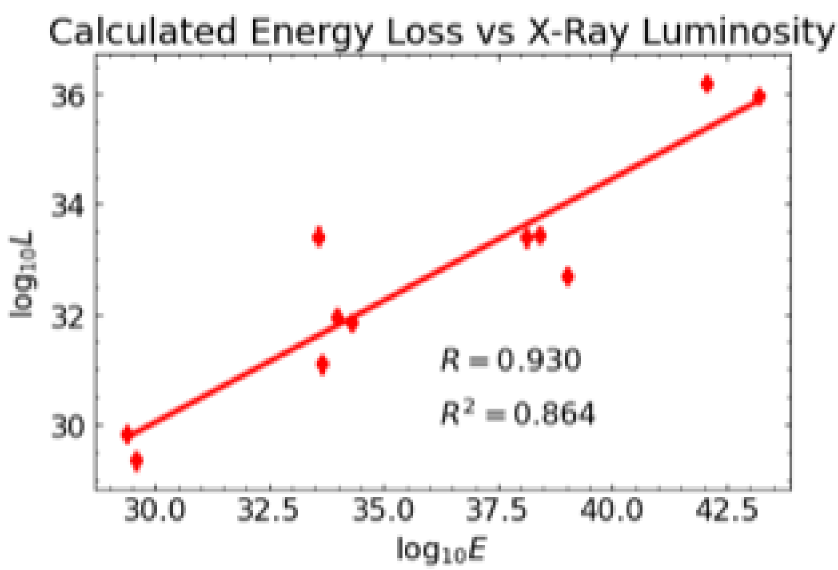

Figure 6: Calculated Spin down luminosities and Observed luminosities in the X-ray band. High correlation values indicates a good fit and that the pulsar is powering its surrounding PWNe

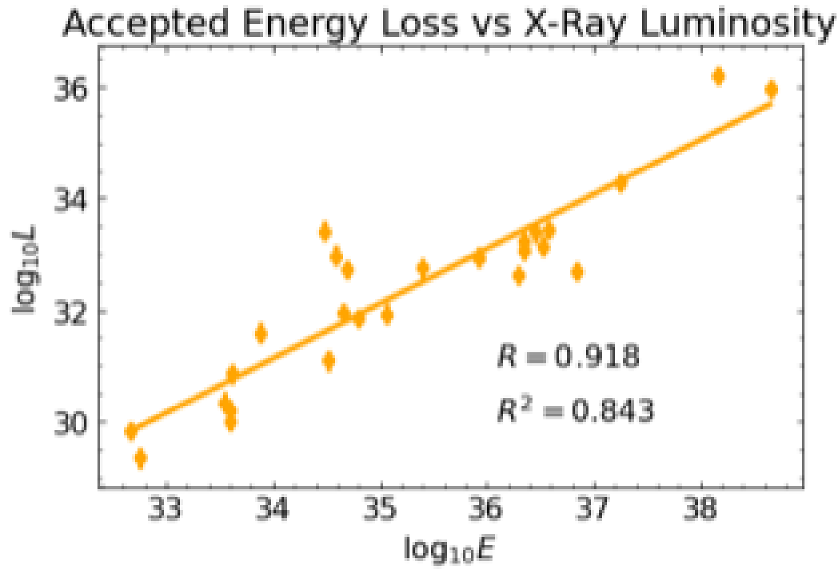

Figure 7: Accepted (i.e. observed from the pulsar) luminosities and the X-Ray Luminosity of the surrounding PWN. This data set has a relatively high R^2 and slope compared to other data sets examined.

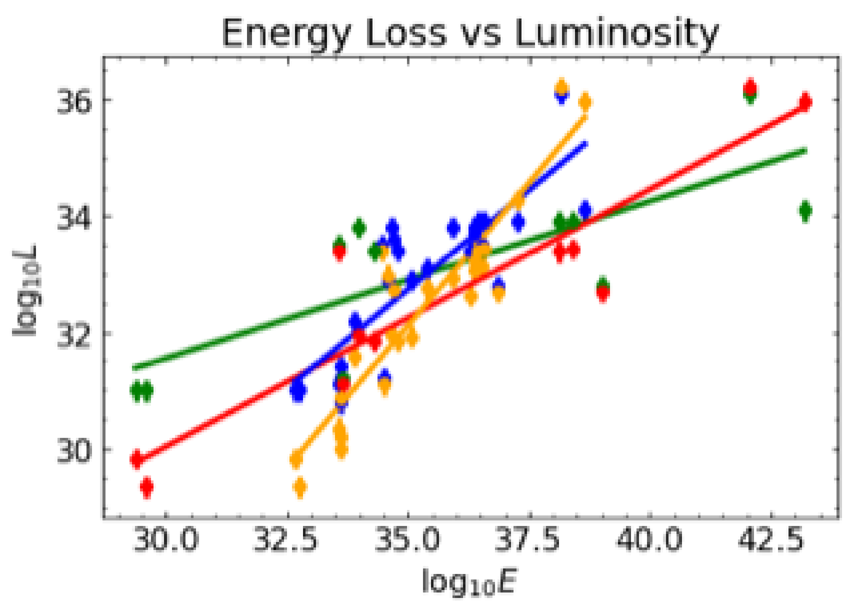

Figure 8: Energy loss from spin down luminosity and observed luminosity of PWNe. The colors correspond to figures 4, 5, 7, and 8. Each trend is roughly linear, but with decidedly different slopes and correlations.

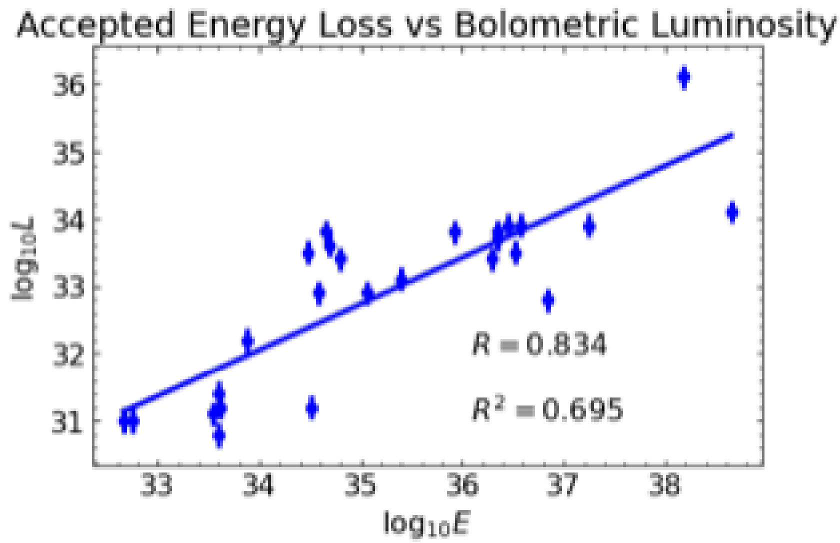

Figure 9: Accepted (i.e. observed from the pulsar) luminosities and the X-Ray Luminosity of the surrounding PWN.

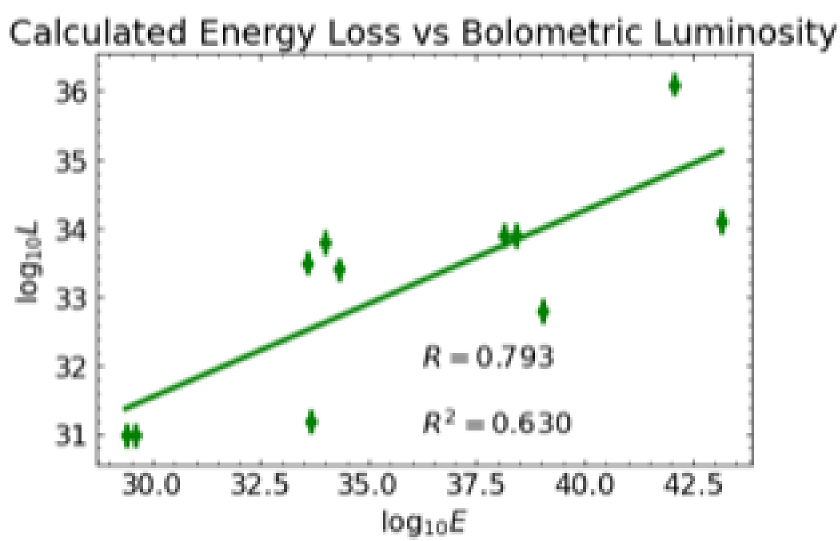

Figure 10: Calculated Energy loss and observed Bolometric Luminosities of PWNe and their respective pulsars. The trend is definitely linear, but the correlation value is low, indicating there is more physics going on than just spin down luminosity.

Graph	Slope	y-intercept	R^2
Calculated and Bolometric	0.271	23.43	0.63
Calculated and X-Ray	0.44	16.73	0.86
Accepted and Bolometric	0.684	8.79	0.70
Accepted and X-Ray	0.981	-2.24	0.843

Table 1: Data sets, and the resulting lines of best fit for Energy Loss of the Pulsar and Observed Luminosity of the PWN surrounding it. See figs 5 to 9 for graphs and more details on each data set. All the slopes being < 1 shows how pulsars do not fully power the surrounding PWN.

F0	F1	Energy	Source
3e-10	2e-18	1.278896833e-17	lwy+16
1e-6	2e-15	5.95163110e-14	ljg+15
7e-10	8e-17	1.58184379e-15	fak15
35e-12	81e-20	3.41628126e-18	jh05
9e-11	3e-19	5.65332644e-19	hlk+04
5e-10	2e-15	2.23892920e-14	dml02
14e-12	4e-20	1.58062005e-19	hlk+04
2e-11	1e-18	5.07318561e-18	jbv+19
2e-11	9e-19	8.86800275e-18	ywml10
7e-10	5e-18	1.26479778e-16	hlk+04
2e-11	3e-18	6.05606514e-18	ymw+10

Table 2: Frequencies and derived values of spin down luminosity. F0 refers to the current frequency of the pulsar,and F1 to the derivative of the frequency. Frequencies are given in units of 1/s and Luminosity in erg/s.

This source of error is not accounted for in the quantitative error analysis. The error on the luminosity is significant, but still cannot account for the difference between the observed luminosity and the theoretical spin down luminosity. This is only one small part of the total picture, however.

Fig 8 shows the majority of our data. We can compare both the trend in bolometric luminosity and x-ray luminosity versus the spin down luminosity of the pulsar. All of the data shows roughly linear trends, supporting the idea that pulsar power PWNe. The Crab Nebula data we took was not included in these data sets.

In fact, we performed a linear fit on the data to examine the relationship between calculated spin down luminosities to observed values. The fits over the various data sets considered can be found in table 2. A list of frequencies and Luminosities can be found in table 3.

Looking at the fits, each data set shows a roughly linear relationship between Spin Down or Pulsar Luminosity and PWN luminosity. The slopes of these linear fits differ greatly. The fits vary from having a slope of 0.271 to a slope of 0.981. It is important to note the differences in R^2 statistic across the linear fits as well. While all are roughly linear, Fig.4 has significantly higher correlation value than fig. 8. This may reveal issues with our model's assumptions. These results are an interesting supplement to the data we took ourselves. The roughly linear relationship across the graphs show how there is a correlation between spin down luminosity and PWN luminosity even if it is not a simple relationship.

4 Discussion

Comparing our observed total luminosity in the Crab Nebula with the spin down luminosity gives a difference of several orders of magnitude. This significant difference between observed and theoretical luminosities is not shocking. As shown in [14] spin down energy loss is not the entire picture when it comes to powering the pulsar. Additionally, there were most likely significant systematic errors in our calculation. Some of these errors came from inital data collection. There were several stars inside of the wind nebula that were also incidentally included in the mask. Additionally, the rather low s/n ratio meant the random error is high. This well represented by the fact our error was nearly half an order of magnitude. Using a blackbody model undoubtedly introduced more error - systematic error from the model simplification and random error from the color temperature calculation. This much error means our value for luminosity can be trusted as an order of magnitude estimation at best. Overall, these sources of error lead to an untrustworthy luminosity value. Given the already high reliance on outside sources, it is disappointing the direct calculation of Luminosity turned out so poor. If time and money were not constraints on this project, we would have measured the value of the flux over a broad range of wavelengths to get a more accurate measurement of bolometric luminosity. The process was still interesting, however, and showed how individually small errors can add together to produce massive errors after processing. It shows the importance of carefully controlling error in astrophysical research. This part of the project also serves as an interesting proof-of-concept for how these luminosity calculations can be done.

Using external data sets which have much more accurate and precise data is a good way to fix this issue. As shown in fig 5 to 9 it does appear that the energy lost from the pulsar is what is causing the wind nebulae to grow. This is further indication that the pulsars are 'powering' the wind nebula's that are around them. This claim is supported by the relatively low uncertainties on the luminosity figures, making the fits and resulting conclusions more accurate than the calculation of the Crab Nebula luminosity. Additionally, while this data is far more accurate than the Luminosities we calculated ourselves, it is still clearly not quite the same as the spin down luminosities. This is indicated by the fact the slopes are not all one. There are most likely unaccounted for energy transfer mechanisms.

The difference between figure 8 and figure 4 is also important to note. The R^2 value for the x-ray band is higher, and the slope is steeper than for the values looking at bolometric luminosity. The stronger correlation from the x-ray band indicates that the energy from the pulsar is not evenly distributed over all wavelength bands which are radiated. The peak at high energies should not surprising, however, given Fig 1. The difference in proportionality values across the data sets was surprising as the differences were large (0.27 - 0.98).

It is interesting to note the slope between the Accepted Luminosity and the measured PWN luminosity is almost exactly one. This further highlights the special significance of the x-ray band. This relationship is interesting to compare to previous studies. As shown in [3] there should be a strong proportionality between spin down luminosity and regular luminosity. They also noted this relationship is particularly strong when only observing the x-ray band. In particular, they found this to be caused by the co-rotation of the pulsar's magnosphere around the pulsar itself. Their results regarding the higher correlation in the x-ray band alings with our findings and may explain the differences in correlation between the bolometric luminosity and the x-ray luminosity. More detailed examination of this would be required to fully understand the causes and implications. It is also important to note that the slope and R^2 values for the Accepted Luminosity shows a stronger correlation between the pulsar's energy loss and the PWN's gain in energy. This indicates the dominant source of our systematic error comes not from our assumption that the PWN is absorbing most of the energy from its enclosed pulsar, but from our simplistic model of spin down Luminosity. Since we can see the energy in compared to the energy out (particularly for the Accepted and x-ray data) is lower than for the calculated luminosities.

Getting a more accurate picture of pulsar energy loss could significantly close the gap between the two luminosity values. Additionally, The observation that the spectrum is more heavily weighted towards the x-ray band may explain why the estimation of the luminosity of the Crab Nebula was low; the wavelength bands we were looking at were much lower energy. So, they take up disproportionately too little of the crab nebula spectrum when compared with a black body.

While the relationship between the slowing of the rotation of the Pulsar and the surrounding PWN is clearly present experimentally, there are still significant differences. Some of these differences come form experimental errors. Many of these errors - mostly in the direct luminosity calculation - could have easily been fixed by an improvement in equipment. For example, having access to more filters or our own spectrometer would have been very useful. This would have not only limited errors, but also allowed us to more accurately estimated what those errors were. For the future, it also would be helpful to have an improved PWN model. From the fit we performed, it is evident that there are other sources of PWN luminosity besides spin down effects. Including other effects - like perhaps direct radiation of the shocked gas - would improve the discrepancy in the model. Our study still serves as a proof of concept and reasonable evidence of how Pulsars are the engines of their surrounding nebulae.

5 Acknowledgements

I would like to thank Joe Politi and Hudson Powell for working on this project with me. I would also like to thank Dr. Lubin and Jeonghwa Kim for their guidance and instruction throughout the process.

References

[1] H. Abdalla, A. Abramowski, F. Aharonian, F. Ait Benkhali, A. G. Akhperjanian, T. Andersson, E. O. Angüner, M. Arrieta, P. Aubert, et al. The population of TeV pulsar wind nebulae in the h.e.s.s. galactic plane survey. *Astronomy &amp Astrophysics*, 612:A2, apr 2018.

[2] Walter Baade and Fritz Zwicky. Cosmic rays from super-novae. *Proceedings of the National Academy of Sciences*, 20(5):259–263, 1934.

[3] Werner Becker and Joachim Trümper. The x-ray luminosity of rotation-powered neutron stars. *arXiv preprint astro-ph/9708169*, 1997.

[4] MS Bessell, F Castelli, and Bertrand Plez. Model atmospheres broad-band colors, bolometric corrections and temperature calibrations for o-m stars. *Astronomy and astrophysics*, 333:231–250, 1998.

[5] R Buehler, JD Scargle, RD Blandford, Luca Baldini, MG Baring, A Belfiore, E Charles, J Chiang, F D'ammando, CD Dermer, et al. Gamma-ray activity in the crab nebula: the exceptional flare of 2011 april. *The Astrophysical Journal*, 749(1):26, 2012.

[6] KS Cheng, Ronald E Taam, and W Wang. Pulsar wind nebulae and the x-ray emission of nonaccreting neutron stars. *The Astrophysical Journal*, 617(1):480, 2004.

[7] James Condon and Scott Ransom. Chapter 6: Pulsars. Oct 2015.

[8] Bryan M Gaensler and Patrick O Slane. The evolution and structure of pulsar wind nebulae. *arXiv preprint astro-ph/0601081*, 2006.

[9] A Hewish, SJ Bell, JDH Pilkington, PF Scott, and RA Collins. Observation of a rapidly pulsating radio source (reprinted from nature, february 24, 1968). *Nature*, 224(5218):472, 1969.

[10] Oleg Kargaltsev, Benoît Cerutti, Yuri Lyubarsky, and Edoardo Striani. Pulsar-wind nebulae. *Space Science Reviews*, 191(1):391–439, 2015.

[11] D. R. Lorimer and M. Kramer. *Handbook of Pulsar Astronomy*, volume 4. 2004.

[12] R N Manchester, G B Hobbs, A Teoh, and M_ Hobbs. The australia telescope national facility pulsar catalogue. *The Astronomical Journal*, 129(4):1993, 2005.

[13] R Minkowski. The crab nebula. *The Astrophysical Journal*, 96:199, 1942.

[14] Andrea Possenti, Rossella Cerutti, Monica Colpi, and Sandro Mereghetti. Re-examining the x-ray versus spin-down luminosity correlation of rotation powered pulsars. *Astronomy & Astrophysics*, 387(3):993–1002, 2002.

[15] Milton Ruiz, Vasileios Paschalidis, and Stuart L Shapiro. Pulsar spin-down luminosity: Simulations in general relativity. *Physical Review D*, 89(8):084045, 2014.

[16] Maki Sekiguchi and Masataka Fukugita. A study of the b- v color-temperature relation. *The Astronomical Journal*, 120(2):1072, 2000.

[17] Frederick D Seward and Zhen-Ru Wang. Pulsars, x-ray synchrotron nebulae, and guest stars. *The Astrophysical Journal*, 332:199–205, 1988.

[18] D Volpi, L Del Zanna, E Amato, and N Bucciantini. Non-thermal emission from relativistic mhd simulations of pulsar wind nebulae: from synchrotron to inverse compton. *Astronomy & Astrophysics*, 485(2):337–349, 2008.

[19] M. Wenger, F. Ochsenbein, D. Egret, P. Dubois, F. Bonnarel, S. Borde, F. Genova, G. Jasniewicz, S. Laloë, S. Lesteven, and R. Monier. The SIMBAD astronomical database. *Astronomy and Astrophysics Supplement Series*, 143(1):9–22, apr 2000.

[20] Qiang Yuan, Peng-Fei Yin, Xue-Feng Wu, Xiao-Jun Bi, Siming Liu, and Bing Zhang. A statistical model for the γ-ray variability of the crab nebula. *The Astrophysical Journal Letters*, 730(2):L15, 2011.